The case for multiband sensing

Shridhar Mubaraq Mishra
EECS Department
UC Berkeley
Email: smm@eecs.berkeley.edu

Rahul Tandra
EECS Department
UC Berkeley
Email: tandra@eecs.berkeley.edu

Anant Sahai
EECS Department
UC Berkeley
Email: sahai@eecs.berkeley.edu

***Abstract*— Cognitive radios achieve opportunistic use of underutilized spectrum by sensing and using frequency bands only if no primary user is detected. Previous approaches to spectrum sensing have examined one band at a time. We argue that this ignores the sparsity inherent to the problem: not only are a large fraction of bands unused, but the number of primary antenna sites is far smaller than the number of occupied bands due to the expense of towers. Exploiting this sparsity leads to better performance and more robustness to fading models.**

Fading consists of two major components: multipath and shadowing. Multipath can be counted on to be qualitatively independent across both frequencies and space. Shadowing has an uncertain distribution that is not guaranteed to be independent across space, but it can be counted on to not be very frequency selective. Multiband sensing leverages this to reduce the impact of the shadowing uncertainty on the non-interference guarantee given to the primary users. Finally, cooperation can behave qualitatively differently from cooperation. While cooperation among singleband sensors is needed to meet a target probability of harmful interference to others, cooperation for multiband sensors can be used instead to reduce the probability of missed opportunity for ourselves.

I. Introduction

The current model of spectrum allocation and licensing leads to systematic underutilization of the spectrum. In most locations and at most times, most bands are effectively unused [1], [2]. The consensus is that the underlying cause is a lack of flexibility in the current regulatory model. There are two important dimensions of flexibility. Flexibility of use refers to the ability of spectrum licensees to choose their application, modulation, and coding strategies freely without needing detailed regulatory approval. This allows a licensee to react to consumer demand and take advantage of new technologies. The second dimension is flexibility of spectrum access allowing systems to get access to additional spectrum as needed without having to go through the government regulators.[1] The key consideration is to avoid causing harmful interference to other users. The idea is to shift the objective of peaceful coexistence from being considered purely at the "regulatory layer" to something that is addressed at runtime by wireless systems themselves. The big open question is to determine how this should be done.

There are three broad approaches to opening up spectrum access: underlay, secondary markets, and opportunistic use. The underlay approach (UWB) attempts to avoid harmful interference by specifying a very low spectral mask for transmitted power [3]. This approach is overly conservative for the realistic case when most bands are empty.

The secondary markets approach is that wireless systems should get explicit permission from primary license holders in order to use those bands, presumably after paying them something. While markets are a good way of allocating a scarce resource, the major problem with this approach is that it does not address the current issue of unused spectrum that cannot be accessed. *If a primary licensee has not bothered to deploy its own system somewhere, there is no reason to suppose that it would deploy a special system to negotiate and grant access for others in those areas!* [2] Because primary system operators do not want to give birth to their own future competitors, there is a further disincentive for deploying such market systems.

Cognitive radios aim to enable the opportunistic use of spectrum by secondary users who promise to sense the presence of the primary user[3] and only use the band once it is deemed empty. The primary user cannot be counted on to participate in this process. Hence cognitive radios must make the non-interference guarantees on their own, as well as bear the cost of any system complexity required. Along with providing guarantees to the primary, the cognitive radio must also maximize its own system's ability to detect spectral opportunities and utilize them as needed. Unfortunately, there is an inherent tension[4] between guarantees to the primary and the ability to detect spectral opportunities. Our goal in this paper is to investigate sensing approaches that attempt to alleviate this tension. If the secondary system makes overly optimistic assumptions about its ability to sense primaries, it is the primary systems' users that must suffer. This makes the operators of primary systems understandably sceptical of the promises made by secondary systems. Thus, the non-interference guarantees must be provided under minimalist models that must hold regardless of the specific environment in which the secondary systems happen to be deployed. In contrast, improved detection of spectral opportunities benefits

[1]The technological prerequisite for such dynamic spectrum access is a degree of frequency agility in the radios.

[2]Specifically, such areas are likely areas of very low spectrum utilization and hence areas in which the market-clearing price would be very low. At such a low price, the licensee cannot recoup the fixed cost of negotiation.

[3]A primary user of spectrum has been given a right to use the spectrum for a particular purpose by the appropriate spectrum regulatory agency, e.g. the FCC in the United States

[4]There is also a tension between the flexibility for the primary user and sensing for opportunistic use [4], but that is not the focus of this paper.

the system that is doing the detection and hence there is no intrinsic reason to distrust the details of models.

Guarantees to primary users can be specified by a required probability of harmful interference (P_{HI}). This is the probability that the cognitive radio network is unable to detect an active primary user and interferes with this primary. For a network composed of a single radio with the primary signal at a given Signal-to-Noise ratio (SNR), this probability can be bounded by the standard probability of missed detection (P_{MD}) in classical detection theory[5]. But even for detection by a single radio, the required sensitivity for the detector incorporates characteristics of the propagation environment, the assumed density of secondary users, as well as the range and power characteristics of the primary user [5], [6].

For the secondary system, the relevant metric is the probability of missed opportunity (P_{MO}) when a radio does not mark a vacant frequency band as being safe to use.[6] For a single radio, this corresponds to the probability of false alarm (P_{FA}).

An example of such threshold setting can be found in the specifications of the IEEE 802.22 Working Group [7]. The group has defined a detection threshold of -116dBm for individual cognitive radios in the DTV bands — 20dB below the thermal noise floor. Such detection levels can be met in ideal settings with long sensing times. In practice, noise and interference uncertainty limit the radios' ability to detect such low SNR signals [8]–[10]. Under noise uncertainty, low P_{HI} can be achieved only at the cost of increased missed opportunities, i.e., P_{MO} close to 1.

If the desired (P_{HI}, P_{MO}) cannot be met by a single radio, it is natural to consider a cooperative sensing scheme where the primary is declared present if any of the radios can detect it[7] [11]. This reduces the P_{HI} exponentially in the number of cooperating radios. Unfortunately, this kind of cooperation degrades P_{MO} exponentially too. To fight this effect, the P_{FA} on each individual detector must be reduced by making the detector less sensitive. On balance, these two effects can be viewed together as a net win. The reduced sensitivity reflects that we no longer need to accurately model very unlikely deep fades [11]. However, all these cooperative gains rely on a significant degree of fading independence between cognitive radios. While the qualitative[8] independence of multipath is not controversial, the independence of shadowing is difficult to verify. If all radios happen to be indoors, then they all see similar shadowing and the independence assumptions break down. The cooperative gains for P_{HI} are largely wiped out while the probability of missed opportunity remains at the multi-radio level.

To understand our approach to solving this problem, visualize a very simple scenario. There are two cognitive radios trying to detect a TV station – the first radio is on the rooftop while the second is in the basement. The radio in the basement is deeply shadowed and hence cannot reliably detect the primary. This is an example of a 'unqualified' radio. How do we distinguish between a radio on the roof versus a radio in the basement? Intuitively, the radio on the roof can probably see many more primary transmitters (for example it can detect cellular base stations, other TV stations, GPS satellites, etc.). In contrast, the radio in the basement cannot locate any other primary users since all transmissions are deeply shadowed in the basement. Hence, sensing other primary users can help us weed out 'unqualified' radios.

Simultaneously detecting a large number of primary transmitters requires a multiband sensor. The original motivation for multiband sensing came from grabbing vacant frequency bands fast in order to ensure constant spectrum availability [12], or to provide localization using UWB radios [13]. An alternate justification based on group-testing when spectrum utilization is sparse is given in [14]. Our new approach provides a fundamental system level motivation for the same. From the economic perspective, it suggests that investment in infrastructure for spectrum *sensing* naturally enjoys nearly "infinite" economies of scale[9] that are distinct from the finite economies of scale for the deployment of actual communication systems using spectrum. This reality must therefore be reflected in the regulation of spectrum.

The rest of this paper tries to quantify the advantages of multiband sensing. Section II reviews the existing work in a form that makes it easy to understand the results in this paper. With the preliminaries established, Section III develops a model for multiband sensing. This model is justified based on experimental UWB channel modeling data and also incorporates an extreme form of sparsity for primary user sites. Section IV then evaluates the performance of a single multiband spectrum sensor. Section V discusses the interaction of multiband sensing with cooperation. Finally, Section VI

[5]This bound assumes that a radio that does not detect the primary will always interfere with it.

[6]Note, there is no need for the radio to actually use this band. But the role of spectrum sensing is to provide the secondary system the opportunity to use the band if needed.

[7]We call this the "OR" rule for cooperation. In general for a system of N radios, we can have a rule that declares a primary present if at least k of the radios say that the primary is present

[8]There is a technical issue here. The qualitative feature required is that if one radio has an unfortunately deep multipath fade at a particular frequency, then the probability of other spatially separated radios also having deep fades is an event whose probability is exponentially rare. This is true. The multipath fading random variables themselves might not be independent because it is the poorly modeled shadowing that determines whether there is a line of sight path, etc. However, if such direct paths exist, very deep multipath fades are impossible. Essentially what can be trusted is that conditioned on the the values for the gains on the various signal paths, the phases remain iid uniform random variables across paths and radios.

[9]In that it is easier and safer to determine the collective occupancy of many bands together than it is to answer the question individually for each band separately.

closes the paper with a view towards future work.

II. Preliminaries

A. Performance metrics

The energy detector[10] is used as an illustrative example though the results of this paper are valid for other detectors too (e.g. coherent detectors and feature detectors).

The goal is to distinguish between the following hypothesis:

$$\begin{aligned}\mathcal{H}_0 : Y[n] = &\quad W[n] &\quad n = 1, \ldots, M\\ \mathcal{H}_1 : Y[n] = &\quad X[n] + W[n] &\quad n = 1, \ldots, M\end{aligned}$$

At first, for convenience assume that all $W[n]$ are independent and distributed as $\mathcal{N}(0, \sigma_w^2)$. Furthermore all $X[n]$ are independent and distributed as $\mathcal{N}(0, \sigma_s^2)$. M is the number of samples.

The detection rule for energy detection is:

$$\frac{1}{M}\sum_{j=1}^{M} Y[n]^2 \underset{H_0}{\overset{H_s}{\gtrless}} \lambda \tag{1}$$

For each λ we get a curve for probability of detection versus SNR as shown in Figure 1.

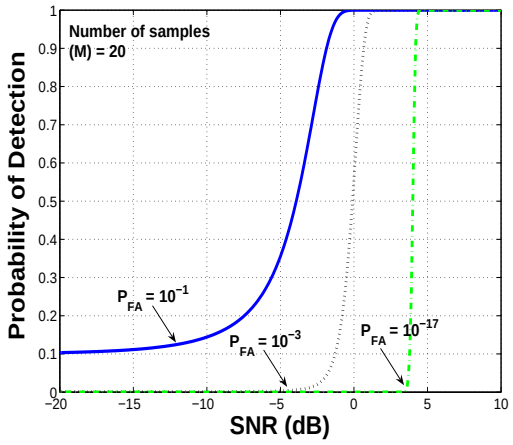

Fig. 1. Probability of detection as a function of SNR for various values of probability of false alarm.

Next we consider the distribution of the channel fades. Let $F_\Gamma(\gamma)$ be the distribution function of the SNR. Then the average P_{HI} is (assuming a single radio, see [11] for the required scaling with multiple radio systems):

$$P_{HI} = \int P_{MD}(\gamma)\, dF_\Gamma(\gamma). \tag{2}$$

[10]The energy detector has the additional advantage of preserving the maximum flexibility of use for the primary user since it does not rely on any knowledge of the primary's modulation scheme.

B. Noise uncertainty

So far, we assumed that the noise is white Gaussian and its variance (σ_w^2) is completely known. However, in reality this is only an approximation. There is always some residual uncertainty for which we cannot fit a statistical model. A detailed model for noise uncertainty and its effect on detector performance is given in [8], [9]. In this paper, a simple model for noise uncertainty suffices for the energy detector. We assume that the noise process $W[.]$ is a zero mean white Gaussian process with variance $\sigma_w^2 \in [\sigma_{low}^2, \sigma_{high}^2]$.

Thus, the relevant worst case performance is

$$P_{FA} = Q\left(\frac{\lambda - \sigma_{high}^2}{\sqrt{\frac{2}{M}}\sigma_{high}^2}\right) \tag{3}$$

$$P_{MD}(\gamma) = 1 - Q\left(\frac{\frac{\lambda}{\sigma_{low}^2} - (1 + 10^{\frac{\gamma}{10}})}{\sqrt{\frac{2}{M}}(1 + 10^{\frac{\gamma}{10}})}\right). \tag{4}$$

C. The propagation environment

The received SNR (γ) is modeled as

$$\gamma = \left(P_t - (L + MP + S) - 10\log_{10}(\sigma_w^2)\right) \tag{5}$$

where P_t is the transmit power in dBm and σ_w^2 is noise power in mW.

Distance dependent path loss L**:** Path loss forms the most significant portion of energy loss in the wireless propagation environment [15]. This is what we are trying to lower bound [5].

Shadowing S**:** Shadowing arises from the absorption of radio waves by obstacles. For the purpose of tractability, shadowing on the log scale has been assumed to be normally distributed [15] based on the application of Central Limit Theorem to a large number of small absorptive losses.

Multipath MP**:** Multipath arises due to the constructive or destructive addition of radio waves at the receiver [16]. Multipath at the same receiver is very different for different frequencies since the relative phase differences along different physical paths are now different. Here we assume multipath to be log normal purely to make the analysis easier. However the results remain qualitatively the same even when multipath is assumed to be Rayleigh or Ricean as is standard [16].

D. Single radio performance and tradeoffs

Figure 2 shows the P_{MO} versus P_{HI} curve for an energy detector for a fixed SNR (-6dB). If we knew the distribution of the SNR then we could plot the average P_{MO} versus P_{HI} curve which is the best P_{MO} versus P_{HI} tradeoff curve in Figure 2.

Next, Figure 3 plots the curve assuming a nominal noise power of -96 dBm and a uncertainty of 1 dB. In this case we see that the performance at low P_{HI} is significantly worse as compared to completely known noise statistics. To achieve low P_{HI} we are forced to set the detector threshold within the noise uncertainty region. For this detector threshold the worst

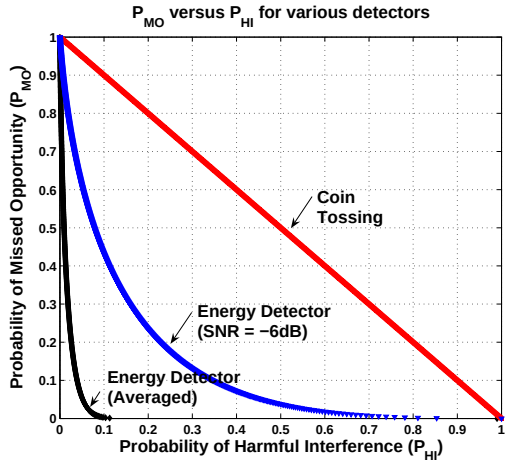

Fig. 2. Performance characteristics of a various detectors for a single radio. A coin-tossing detector does not require any physical measurements and hence gives the worst possible tradeoff between P_{MO} and P_{HI}. The average performance is much better than the performance for deep fades (E.g. -6 dB SNR).

case P_{MO} is much higher since the noise alone can cause it to trigger.

The dotted black curve in Figure 3 is the convex hull of the set of all achievable points for singleband detection with noise uncertainty. At low P_{HI} "time-sharing"[11] dominates the actual detector.

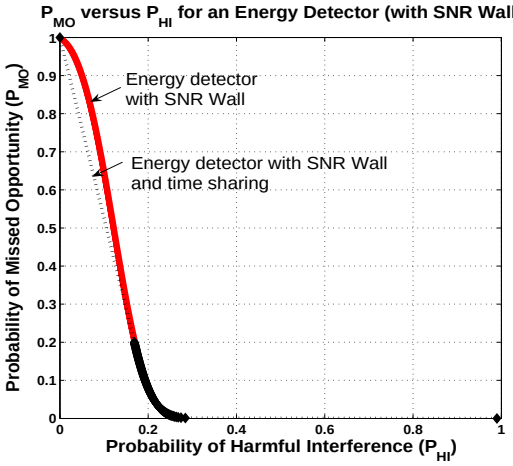

Fig. 3. Average performance characteristics of the energy detector with noise uncertainty of 1 dB. P_{MO} in this curve is obtained from equation (3) and P_{HI} was obtained by averaging P_{MD} in equation (4) over the SNR distribution.

E. Performance of cooperating radios

The most conservative cooperation rule (obtaining the lowest P_{HI}) is the "OR" rule, i.e., we declare that the primary is present for the system if any of the cognitive radios declares that the primary is present. In this section we consider the "OR" rule for cooperation. Analogous expressions for other rules like the 'k out of N' rules[12] can also be derived.

$$\begin{aligned} P^s_{HI} &= \int \prod_{i=1}^{N} P_{MD}(\gamma_i) dF_{\Gamma_1^N}(\gamma_1, \ldots, \gamma_N) \\ &= \mathbb{E}\left[\prod_{i=1}^{N} P_{MD}(\Gamma_i)\right] \end{aligned}$$

where Γ_i is the random variable denoting the received SNR at radio i and N is the number of radios. Similarly, the probability of missed opportunity of the system (P^s_{MO}) is given by

$$P^s_{MO} = 1 - [1 - P_{FA}]^N \quad (6)$$

where P_{FA} is the probability of false alarm of the individual radios. To evaluate the performance we need to know the spatial distribution of the received SNR. Here, we consider two extreme cases for spatial distribution.

If the received SNR is spatially independent, then P^s_{HI} can be written as:

$$P^s_{HI} = \{\mathbb{E}[P_{MD}(\Gamma)]\}^N \quad (7)$$

Since P^s_{MO} does not depend on the SNR distribution across space, it remains unchanged. Figure 4 plots the performance of the "OR" rule for different values of N. The curve to the left of the figure corresponds to the case of spatial independence of shadowing. This curve can be obtained by evaluating Eqns. (7) and (6).

We now consider the other extreme, where the received SNR is completely correlated. This corresponds to cases when the cognitive radios are blocked by the same obstacle (the shadowing is completely correlated). The probability of harmful interference in this case can be written as

$$P^s_{HI} = \mathbb{E}\left[(P_{MD}(\Gamma))^N\right] \quad (8)$$

The gain in system P_{HI} is significantly reduced but P_{MO} has been greatly increased. This effect is shown in Figure 4.

III. Towards a model

A. Shadowing correlation across frequencies

In order to verify shadowing correlation across frequencies, we analyzed the measurement data from UWB channel characterization experiments performed by Kunish and Pamp [17].

In Figure 5(a)-(c) the received power on two different frequencies (1 GHz and 1.0625 GHz) is plotted for the LOS, (N)LOS, NLOS configurations. The received power is also plotted after averaging out the multipath. Similarly, Figure 5(d)-(f) show the received power on two frequencies that are further apart (1 GHz and 2 GHz) for LOS, (N)LOS and NLOS configurations. There are a few things to note:

- The range of received power for the LOS configuration is a lot smaller than for other configurations (15dB versus 30dB). Also, multipath is reduced under LOS conditions

[11] These points are obtained by tossing a coin and switching between the corresponding detectors based on the result of the coin toss.

[12] As shown in [11], such other rules tradeoff cooperative gains for robustness to poorly modeled behavior of a fractional subset of nodes.

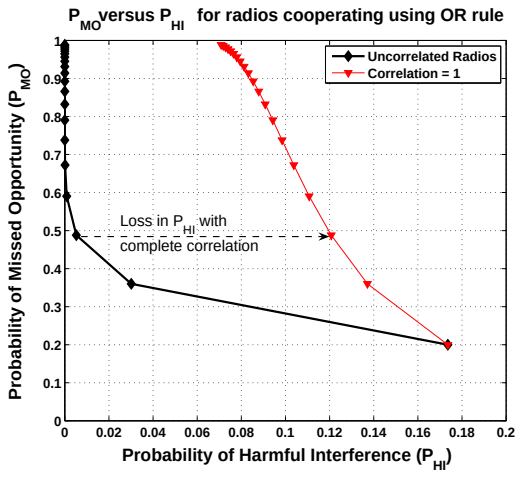

Fig. 4. Performance characteristics of multiple cooperating radios using the OR rule. The P_{HI} performance is very sensitive to the spatial independence assumption of shadowing.

(the multipath is Ricean rather than Rayleigh). Even though the actual correlation between the LOS received powers at the two frequencies is low, we can still make very strong statements about the received power on the second frequency once we have observed the received power on the first frequency. For example, if we see received power (without multipath) on 1 GHz to be above -54dBm, then the chance of seeing the received power on 2 GHz to be below -58dBm is very small.

- The partial LOS ((N)LOS) configuration shows very high correlation as is evident by the nearly diagonal joint density (with the multipath removed). Initially, the transmitter and receiver are in line of sight of each other but that changes as the transmitter is moved. This shows up as increased variability in the multipath.
- Frequencies that are closer together are more correlated than frequencies that are far apart (Compare the correlation between 1GHz and 1.0625GHz, and that between 1GHz and 2GHz). This is probably due to the slow frequency selectivity of building materials in the environment.

B. Co-located primaries

The correlation between frequencies as seen in the previous section is dependent on the fact that the two transmissions are from co-located sources. While this may seem an over simplification, it turns out that multiple primary transmitters often reside on the same tower. In the San Francisco Bay Area there are only a few transmitter locations each of which houses multiple DTV transmitters [18]. For example, the Sutro tower in San Francisco is home to 28 DTV channels including KQED, KTVU and KRON4. Given the large fixed cost of towers, this sparsity of towers relative to frequency bands is something to be generically expected.

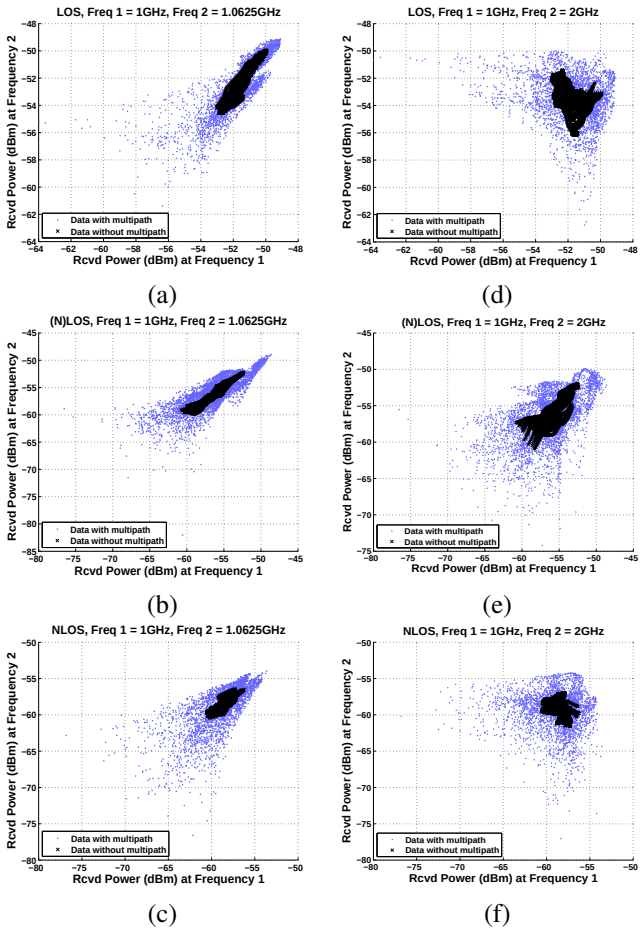

Fig. 5. (a-c) Received power at 1GHz and 1.0625GHz in LOS, (N)LOS and NLOS configurations (d-f) Received power at 1GHz and 2GHz LOS, (N)LOS and NLOS configurations

C. The model

For the analysis in Section IV and Section V, assume that we are trying to detect a primary that is either on or off. Co-located with the primary are other primary transmitters that are always on. These primary users are called 'anchors' – they are always on and their positions with respect to the primary user is also fixed.

Furthermore, assume that the received SNR of the primary and the anchor nodes can be expressed in the form of Equation (5):

$$\begin{aligned} \gamma_P &= \left(P_t - (L + MP_P + S_P) - 10\log_{10}(\sigma_w^2)\right) \\ \gamma_A &= \left(P_t - (L + MP_A + S_A) - 10\log_{10}(\sigma_w^2)\right) \end{aligned}$$

where P_t (the transmit power) is the same for the anchor and the primary, L is the path loss which is also the same for both (assuming they are co-located).

S_P and S_A is the shadowing seen by the primary and the anchor signals respectively. Assume that they are correlated with correlation coefficient ρ, where $0 \leq \rho \leq 1$. Similarly, MP_P and MP_A are the independent multipath. Let $0 \leq \rho' \leq \rho \leq 1$ be the net correlation in fading. Hence for

our discussion, the received powers (in dB) have a normal distribution with mean 3.2 dB and standard deviation 5.5 dB [19].

IV. Performance of multiband sensing

Assume that one anchor and one primary that are co-located. The goal of the cognitive radio is to detect the presence or absence of the primary. To keep things concrete we work with energy detection, i.e., the cognitive radio can measure the energy in both the primary and the anchor band. The question is whether having access to an anchor improves the performance of a single user energy detector.

A. Multiband energy detection

- Run an energy detector for both the primary and anchor bands.
  - Let the number of time samples used for energy detection be M. Let the energy detection thresholds for the primary bands be λ_P and let the corresponding threshold for the anchor bands be λ_A.
  - Compute the empirical estimate of the energy in each band. Let $T(Y_A)$ denote this test-statistic for the anchor, and $T(Y_P)$ be the corresponding test-statistic for the primary band. Now compare these test-statistics to the corresponding thresholds.
  - Let $\mathcal{H}_{P,1}$ denote the decision when the energy estimate in the primary band exceeds λ_P, and $\mathcal{H}_{P,0}$ otherwise. Similarly, declare $\mathcal{H}_{A,1}$ or $\mathcal{H}_{A,0}$ for the anchor band.
- Given the individual decisions in each band, make a global decision of whether the primary is present or absent. This decision is made as shown in Table I. Here $\mathcal{H}_1$ denotes the global decision that the primary band is used and $\mathcal{H}_0$ denotes the global decision that the primary band is empty.

Anchor band decision	$\mathcal{H}_{A,1}$	$\mathcal{H}_{A,1}$	$\mathcal{H}_{A,0}$	$\mathcal{H}_{A,0}$
Primary band decision	$\mathcal{H}_{P,1}$	$\mathcal{H}_{P,0}$	$\mathcal{H}_{P,1}$	$\mathcal{H}_{P,0}$
Global Decision	$\mathcal{H}_1$	$\mathcal{H}_0$	$\mathcal{H}_1$	$\mathcal{H}_1$

TABLE I
MULTIBAND ENERGY DETECTION ALGORITHM

B. Performance analysis of the single anchor multiband detector

For our detector the error probabilities are given by

$$\begin{aligned} P_{HI} &= Prob\left(T(Y_A) > \lambda_A, T(Y_P) < \lambda_P | \text{ Primary is "ON"}\right) \\ P_{MO} &= 1 - Prob\left(T(Y_A) > \lambda_A, T(Y_P) < \lambda_P | \text{ Primary is "OFF"}\right) \end{aligned}$$

If the primary is "ON", harmful interference occurs only if the anchor is seen but not the primary. With relatively small multipath and a high shadowing correlation between the anchor and primary bands, this probability will be very small. Similarly, we manage to find an opportunity if we see the anchor and find the primary band empty. Under the model in Sec. III, we have

$$\begin{aligned} & P_{HI}(\lambda_A, \lambda_P, \rho) \\ = \; & Prob\left(T(Y_A) > \lambda_A, T(Y_P) < \lambda_P | \text{ Primary is "ON"}\right) \\ = \; & \int_{-\infty}^{\infty}\int_{-\infty}^{\infty} P_D(\gamma_A, \lambda_A) P_{MD}(\gamma_P, \lambda_P) \; dF_{\Gamma_A,\Gamma_P}(\gamma_A, \gamma_P) \\ = \; & \mathbb{E}_{F_{\Gamma_A,\Gamma_P}}\left(P_D(\gamma_A, \lambda_A) P_{MD}(\gamma_P, \lambda_P)\right) \end{aligned} \tag{9}$$

and

$$\begin{aligned} & P_{MO}(\lambda_A, \lambda_P, \rho) \\ = \; & 1 - Prob\left(T(Y_A) > \lambda_A, T(Y_P) < \lambda_P | \text{ Primary is "OFF"}\right) \\ = \; & 1 - (1 - P_{FA}(\lambda_P)) \int_{-\infty}^{\infty} P_D(\gamma_A, \lambda_P) \; dF_{\Gamma_A}(\gamma_A) \\ = \; & 1 - (1 - P_{FA}(\lambda_P)) \cdot \; \mathbb{E}_{F_{\Gamma_A}}\left(P_D(\gamma_A, \lambda_P)\right) \end{aligned} \tag{10}$$

where

- $P_{FA}(\lambda)$ — The probability of false-alarm for an energy detector when the detection threshold is λ.
- $P_D(\gamma, \lambda)$ — The probability of detection for energy detection when the signal to noise ratio is γ and the detection threshold is set at λ (See Section II).
- $P_{MD}(\gamma, \lambda) = 1 - P_D(\gamma, \lambda)$.

For any two achievable points (P^1_{HI}, P^1_{MO}) and (P^2_{HI}, P^2_{MO}) we can achieve all points on the line $(\theta P^1_{HI} + (1-\theta)P^2_{HI}, \theta P^1_{MO} + (1-\theta)P^2_{MO})$ joining these two points by randomization according to $0 \le \theta \le 1$. The performance of multiband energy detection for the single anchor case can be characterized by the set of all achievable error probability pairs. Let $\mathbb{R}_{MB}(\rho)$ denote this region for a given frequency correlation coefficient ρ. Formally, we can define this region as

$$\begin{aligned} \mathbb{R}_{MB}(\rho) = \text{Convexhull} \quad \{ \quad & (P_{HI}(\lambda_A, \lambda_P, \rho), P_{MO}(\lambda_A, \lambda_P, \rho)) \\ & : \; 0 \le \lambda_A, \lambda_P \le \infty \} \end{aligned}$$

The multiband energy detector is no worse than the single-band energy detector.

***Theorem** 1:* Let $\mathbb{R}_{NB}$ denote the set of achievable performance points for a single user singleband energy detector. Then, we have

$$\mathbb{R}_{NB} \subseteq \mathbb{R}_{MB}(\rho)$$

for all $0 \le \rho \le 1$.

Proof: For a given primary detection threshold λ_P, let $(P^{NB}_{HI}, P^{NB}_{MO})$ be the error probabilities for the singleband energy detector (See Section II). Similarly, let $(P^{MB}_{HI}, P^{MB}_{MO})$ be the error probabilities for the multiband energy detector (See Eqn. (9), and (10)) using anchor detection threshold λ_A. Setting $\lambda_A = -\infty$, we can easily verify that $P^{MB}_{HI} = P^{NB}_{HI}$ and $P^{MB}_{MO} = P^{NB}_{MO}$. This proves the desired result. ■

C. Characterization of the multiband frontier

In the previous section we defined $\mathbb{R}_{MB}(\rho)$ and used it as a metric to evaluate the performance of multiband detection. Although every point in the region $\mathbb{R}_{MB}(\rho)$ is achievable, the interesting performance points are the Pareto optimal points. Pareto optimal points are defined as those points in $\mathbb{R}_{MB}(\rho)$

which are better than every other point in the region in at least one coordinate. We call this set of Pareto optimal points the multiband performance frontier and denote it by $\mathbb{F}_{MB}(\rho)$. Note that by definition $\mathbb{F}_{MB}(\rho)$ is convex and $(0,1)$ and $(1,0)$ are the end points of this curve.

Figure 6 compares the single anchor multiband energy detector performance with the narrow band energy detector performance. The solid black curve is the frontier $\mathbb{F}_{MB}(\rho)$ for multiband detection and the dotted black curve is the frontier for singleband energy detection with time-sharing. From the figure it is clear that the multiband energy detector outperforms singleband energy detector. In particular, the slope of the frontier at $(0,1)$ is infinite for multiband detection as compared to a constant for singleband detection. This means that we can achieve very low P_{HI} requirements for moderate values of P_{MO}. The above claim follows directly from the following theorem.

***Theorem** 2:* The slope of the frontier $\mathbb{F}_{MB}(\rho)$ at the $(0,1)$ point is ∞.

Proof: We omit the proof here for space constraints. ■

Figure 6 also points out an interesting aspect of the frontier $\mathbb{F}_{MB}(\rho)$. For a given λ_P, let $F_{\lambda_P}(\rho)$ denote the locus of points $(P_{HI}(\lambda_A,\lambda_P,\rho), P_{MO}(\lambda_A,\lambda_P,\rho))$ as λ_A varies from 0 to ∞. Figure 6 also plots $F_{\lambda_P}(\rho)$ for three different values of λ_P (consequently different values of P_{FA}^P as labeled in the figure). From the figure we can see that each of the three curves partially overlap with the frontier $\mathbb{F}_{MB}(\rho)$. This suggests that the Pareto optimal frontier is the envelope of the family of curves $F_{\lambda_P}(\rho)$ as λ_P varies from 0 to ∞.

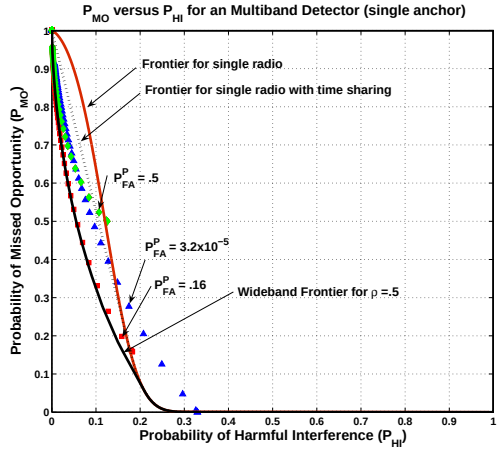

Fig. 6. Performance characteristics of a single multiband radio with a single anchor. The multiband detector outperforms the singleband energy detector. In particular for low P_{HI}, the P_{MO} for the multiband detector is much lower than the P_{MO} for the singleband detector. This can be seen from the slope of the frontiers at $(0,1)$.

D. Robustness of multiband sensing

So far we have shown that multiband energy detection outperforms its singleband counterpart. We now consider the robustness of multiband sensing to the uncertainties in the system: noise level uncertainty, uncertainty in the shadowing distribution, and uncertainty in frequency correlation. Noise level uncertainty was accounted for in our model by assuming that the noise distribution lies an uncertainty set.

For singleband detection, the only way to obtain low P_{HI} is to lower the detection threshold λ_P below σ^2_{high}. However, setting a threshold in the noise uncertainty region adversely affects the system performance in the form of increased P_{MO} (see the single radio frontier in Fig. 6). This is one of the ways that a singleband detector is non-robust to noise uncertainty. For multiband detection, low P_{HI} can be obtained by setting $\lambda_P > \sigma^2_{high}$ and making λ_A sufficiently large. This avoids a catastrophic degradation in P_{MO} to obtain low P_{HI}. Fig. 6 shows that the multiband frontier has slope ∞ for low values of P_{HI}. Physically, this corresponds to demanding a clear view of the anchor before trusting the measurement of the primary. This allows multiband sensing to be more robust to noise level uncertainties as compared to singleband sensing.

In our analysis we assumed that the shadowing is correlated across frequency and that the structure of correlation was completely known, i.e., jointly Gaussian with a correlation coefficient ρ. However, it is unrealistic to assume complete knowledge about the shadowing distribution across frequency. How does the performance vary as we move away from the completely known model?

Robustness can be analyzed by assuming that the joint distribution is known only to a few quantiles. The complete analysis of this model is not done here due to space constraints. Here, the robustness of multiband detection is considered to uncertainty in the frequency correlation coefficient ρ. Assume that the shadowing distribution across frequency is jointly Gaussian, with the frequency correlation coefficient $\rho \in [\rho_{low}, \rho_{high}]$. Under this uncertainty model, the worst case performance is relevant. It turns out that the multiband detector performs at least as well as the detector with frequency correlation ρ_{low}.

***Theorem** 3:* Let $0 \le \rho_1 < \rho_2 \le 1$ be given. Then

$$\mathbb{R}_{MB}(\rho_1) \subset \mathbb{R}_{MB}(\rho_2)$$

where $A \subset B$ means that A is a proper subset of B.

Proof: We omit the proof for space constraints. ■

Figure 7 plots the multiband frontier for different values of ρ. This numerically verifies the statement of Theorem 3.

V. Cooperation among multiband radios

This section considers a system of N radios each of which runs the multiband energy detector described in Section IV. The radios cooperate to decide whether the primary band is used or empty. Assume also that each of the radios in the system are homogeneous, i.e., the detection thresholds λ_A and λ_P are same for all the radios in the system.

As a baseline, consider the strict "OR" rule in which the system decides that the primary band is vacant iff each of the individual radios declare that the band is vacant. Recall that each of the individual radio is running a multiband energy detector, which means that they declare the primary band

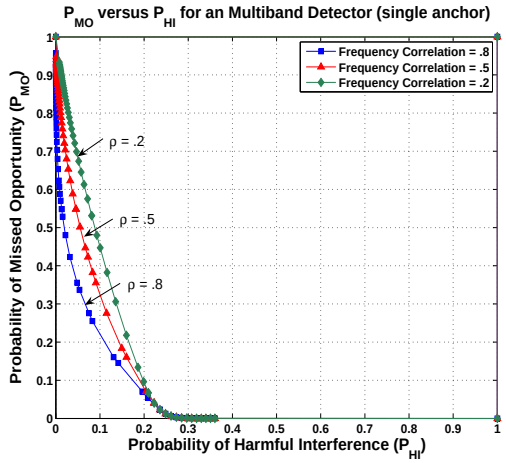

Fig. 7. Performance characteristics of a single multiband radio as the frequency correlation coefficient ρ varies. The achievable region strictly grows as the frequency correlation increases.

empty iff they detect the anchor and find the primary band empty. Under this rule the probability of harmful interference of the system is given by

$$P_{HI}^{s,MB} = \mathbb{E}\left[\prod_{i=1}^{N} P_D(\Gamma_{A_i}) \cdot P_{MD}(\Gamma_{P_i})\right]$$

Here the expectation is over the random variables $(\Gamma_{A_1}, \Gamma_{P_1}, \cdots, \Gamma_{A_N}, \Gamma_{P_N})$, where Γ_{A_i} is the SNR of the anchor signal at the ith radio, and Γ_{P_i} is the SNR of the primary signal at the ith radio. As in Section IV, $P_D(\gamma)$ is the probability of detection as a function of the signal to noise ratio γ and $P_{MD}(\gamma) = 1 - P_D(\gamma)$.

Similarly, the probability of missed opportunity of the system is given by

$$P_{MO}^{s,MB} = 1 - \mathbb{E}\left[\prod_{i=1}^{N} P_D(\Gamma_{A_i})\right] \cdot (1 - P_{FA}^{P})^N.$$

The above equations reveal that the gains from cooperation for this baseline are exactly the same as discussed in Section II-E. In particular,

- $P_{HI}^{s,MB}$ decreases as N increases.
- $P_{MO}^{s,MB}$ increases as N increases.

A. Multiband energy detection with abstention

Recall that the multiband energy detection algorithm in Section IV-A declared that the primary is present when the radio fails to detect the anchor. The reasoning behind this was the following: if the radio does not see the anchor which is always "ON" then it is most likely deeply shadowed to the primary too. Since a deeply shadowed radio's detection results are unreliable, being conservative requires declaring that the primary might be "ON".

The above discussion suggests a way to weed out deeply shadowed radios. We introduce a ternary decision scheme, i.e., the radio declares one of the following three decisions: $\mathcal{H}_1$ – the primary is present, $\mathcal{H}_0$ – the primary is absent and $\mathcal{A}$ – the primary abstains from making any decision. The modified detection algorithm is summarized in Table II.

Anchor band decision	$\mathcal{H}_{A,1}$	$\mathcal{H}_{A,1}$	$\mathcal{H}_{A,0}$	$\mathcal{H}_{A,0}$
Primary band decision	$\mathcal{H}_{P,1}$	$\mathcal{H}_{P,0}$	$\mathcal{H}_{P,1}$	$\mathcal{H}_{P,0}$
Global Decision	$\mathcal{H}_1$	$\mathcal{H}_0$	$\mathcal{A}$	$\mathcal{A}$

TABLE II
MODIFIED MULTIBAND ENERGY DETECTION ALGORITHM

Given that each radio makes a ternary decision, the "OR" rule for cooperation is modified as follows: the system declares that the band is safe to use iff each of the qualified radio (radios that do not abstain) declares that the primary is absent. If all the radios abstain or any radio votes that the primary is present, then the system declares that the primary band is unsafe.

We now derive the performance of this modified "OR" rule for cooperation. For a given i, define S_i to be the set of all subsets of $\{1, 2, \cdots, N\}$ of cardinality i. For each $\mathbf{u} \in S_i$, define $\hat{\mathbf{u}} = \{1, 2, \cdots, N\} \setminus \mathbf{u}$.

The harmful interference event can be written as a disjoint sum of events parametrized by the number of abstaining users, $i = 0, 1, \cdots, N-1$. By the above definitions S_i denotes the set of possible combinations of i abstaining radios. Also, if $\mathbf{u}$ denotes the set of radios that abstain, then $\hat{\mathbf{u}}$ denotes the radios that don't abstain.

For a given $\mathbf{u} \in S_i$, let $\mathbb{P}_A(\mathbf{u})$ denote the probability that the radios in the set $\mathbf{u}$ abstain and let $\mathbb{P}_{MD}(\hat{\mathbf{u}})$ denote the probability that the radios in the set $\hat{\mathbf{u}}$ mis-detect the primary. By definition we have

$$\begin{aligned}\mathbb{P}_A(\mathbf{u}) &= \prod_{k=1}^{i} P_{MD}(\gamma_{A_{u(k)}}) \\ \mathbb{P}_{MD}(\hat{\mathbf{u}}) &= \prod_{k=1}^{N-i} P_D(\gamma_{A_{\hat{u}(k)}}) \cdot P_{MD}(\gamma_{P_{\hat{u}(k)}})\end{aligned}$$

Using the above notation, the probability of harmful interference can be written as

$$\begin{aligned}\widetilde{P}_{HI}^{s,MB} &= \mathbb{E}\left[\sum_{i=0}^{N-1} \sum_{\mathbf{u}\in S_i} \mathbb{P}_A(\mathbf{u}) \cdot \mathbb{P}_{MD}(\hat{\mathbf{u}})\right] \\ &= \sum_{i=0}^{N-1} \sum_{\mathbf{u}\in S_i} \mathbb{E}\left[\mathbb{P}_A(\mathbf{u}) \cdot \mathbb{P}_{MD}(\hat{\mathbf{u}})\right].\end{aligned}$$

For simplicity, consider the situation where the joint distribution is symmetric. In this case $\mathbb{E}\left[\mathbb{P}_A(\mathbf{u}) \cdot \mathbb{P}_{MD}(\hat{\mathbf{u}})\right]$ is identical for all $\mathbf{u} \in S_i$. Hence, in the symmetrical case the error probabilities can be written as in Equation (11) (since, $|S_i| = \binom{N}{i}$).

If shadowing is spatially uncorrelated, then the above equations become:

$$\begin{aligned}\widetilde{P}_{HI}^{s,MB} &= \sum_{i=0}^{N-1} \binom{N}{i} \mathbb{E}\left[P_{MD}(\Gamma_A)\right]^i \cdot \mathbb{E}\left[P_D(\Gamma_A) \cdot P_{MD}(\Gamma_P)\right]^{N-i} \\ \widetilde{P}_{MO}^{s,MB} &= 1 - \sum_{i=0}^{N-1} \binom{N}{i} \mathbb{E}\left[P_{MD}(\Gamma_A)\right]^i \cdot \mathbb{E}\left[P_D(\Gamma_A)\right]^{N-i} \cdot (1 - P_{FA}^{P})^{N-i}\end{aligned}$$

$$\widetilde{P}_{HI}^{s,MB} = \mathbb{E}\left[\sum_{i=0}^{N-1}\binom{N}{i}\left\{\prod_{k=1}^{i}P_{MD}(\Gamma_{A_k})\right\}\left\{\prod_{k=i+1}^{N}P_D(\Gamma_{A_k})\cdot P_{MD}(\Gamma_{P_k})\right\}\right]$$

$$\widetilde{P}_{MO}^{s,MB} = 1-\mathbb{E}\left[\sum_{i=0}^{N-1}\binom{N}{i}\left\{\prod_{k=1}^{i}P_{MD}(\Gamma_{A_k})\right\}\left\{\prod_{k=i+1}^{N}P_D(\Gamma_{A_k})\cdot(1-P_{FA}^P)\right\}\right] \quad (11)$$

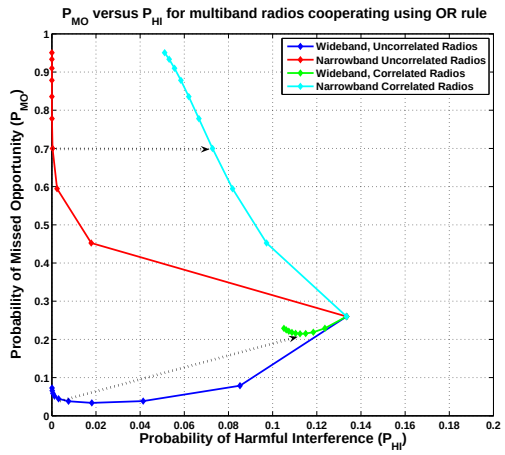

Fig. 8. Impact of voting abstentions on cooperative gains. While the number of cooperating radios is limited, ternary voting provides gains in both P_{HI} and P_{MO} over using the OR rule. This is because ternary voting allows us to weed out 'unqualified' radios from the decision process.

Figure 8 plots the performance of the "OR" rule for cooperation for the case of spatially uncorrelated radios. We start with a single radio performance point P_{HI}, P_{MO} and plot the performance of the system as the number of cooperating radio increases. When the radios do multiband sensing without abstentions P_{HI} drops with cooperation at the cost of increased P_{MO}. With abstentions, *both* P_{HI} and P_{MO} initially drop with an increasing number of cooperating users. P_{MO} then reaches a minimum for a critical number of cooperating users and then increases again after that critical number. This shows that with the abstentions enabled by multiband sensing, we can get significant gains in P_{HI} without losing performance. Intuitively, the early gains from cooperation are due to reducing the probability of having everyone abstain. With many users, this is no longer the dominant source of missed opportunities and the false alarms become significant again.

In plotting these curves we assumed that shadowing is spatially uncorrelated, i.e., the received SNR is independent across space. The figure also shows the loss in performance if the spatial independence assumption is false, i.e., shadowing is completely correlated. In such cases, increasing the number of users is only like increasing the number of samples taken.

We now characterize the critical threshold for the number of cooperating users for which we get the best performance, i.e., least P_{MO}. We know that

$$\begin{aligned}\widetilde{P}_{MO}^{s,MB} &= 1-\sum_{i=0}^{N-1}\binom{N}{i}(1-\beta)^i\cdot[(1-\beta)(1-P_{FA}^P)]^{N-i}\\ &= 1-[(1-\beta)+\beta(1-P_{FA}^P)]^N+(1-\beta)^N\end{aligned}$$

where $\beta = \mathbb{E}[P_D(\Gamma_A)]$. For notational simplicity define $\widetilde{P}_{MO}^{s,MB} =: f(N)$. Minimizing $f(N)$ with N gives us the critical number of cooperating users. Let

$$\bar{N} = \left\lfloor \frac{\log\left[\frac{\log(1-\beta)}{\log[(1-\beta)+\beta(1-P_{FA}^P)]}\right]}{\log\left[\frac{(1-\beta)+\beta(1-P_{FA}^P)}{(1-\beta)}\right]} \right\rfloor$$

Then, the optimal number is given by

$$N^* = \text{argmin}\{f(\bar{N}), f(\bar{N}+1)\}$$

Furthermore, it is clear that the optimal number of cooperating users N^* increases as P_{FA}^P decreases. In practice, the number of cooperating users can be kept at this optimal number by having the most qualified users (those who see the anchors the strongest) vote.

VI. Conclusions

One of the primary areas of cognitive radio research is in device level sensing algorithms that can achieve good sensitivity. All these algorithms either make assumptions about the nature of noise and/or interference when the primary is absent or about synchronization with the primary and coherence times when it is present. Uncertainties about these parameters imposes sensitivity limits on the detector performance.

The naive solution to the problem of sensitivity limited radios is to consider the decision of a variety of radios with the hope that all radios seeing a bad fade is an extremely rare event. Unfortunately, radios cooperating using the OR rule adversely affect their own ability to use opportunities. The main reason for this is the 'every radio is alike' philosophy which does not distinguish between 'qualified' radios (radio that have a good channel to the primary) from 'unqualified' ones.

In this paper we proposed multiband sensing as a mechanism to qualify radios. In the multiband regime, a radio is able to sense many primary transmitters. Taking the co-located 'anchor' (transmitters that are always on) transmitters as an example, we have shown that a multiband radio detecting a single primary and a anchor can greatly increase its achievable region of operation (probability of harmful interference (P_{HI}) versus probability of missed opportunity (P_{MO}) curve). Such a multiband radio does strictly better than a singleband radio.

Furthermore, this achievable region increases as the frequency correlation between the anchor transmitter and the actual primary is increased.

Multiband sensing allows radio to cast their vote using a ternary system (primary present, primary absent, abstain). This enables the system to cooperate only between 'qualified' radios (radios that do not abstain). Under appropriate constraints, ternary voting can lead to better P_{HI} and P_{MO} of the system. Non-zero value of probability of false alarm (P_{FA}) of primary detection limits the number of radios that we can cooperate with, while still getting gains in both P_{HI} and P_{MO}. The situation generalizes easily to when no particular frequency band is designated to be an anchor, but the assumption is that at least some transmitter on the given tower will be on. Even this assumption impacts our own system's P_{MO} and does not take away from the P_{HI} for the primary user.

The path of this work going forward is clear. With the extreme case of transmitter sparsity (a single tower) resolved, the natural next step that we are investigating is to allow multiple towers, but where the number of primary transmitters per tower is large. The idea is to break shadowing down further into two qualitatively distinct components: a directional component that captures the impact of big obstacles like other buildings and a non-directional component that captures the effect of the deployment scenario like indoors, etc. The intuition is that the greatest uncertainty in fading is coming from the non-directional component. This observation, combined with cooperation and clustering should enable us to get results on general case as well.

REFERENCES

[1] "Spectrum policy task force report," Federal Communications Commision, Tech. Rep. 02-135, Nov 2002. [Online]. Available: "http://hraunfoss.fcc.gov/edocs_public/attachmatch/DOC-228542A1.pdf"

[2] "Dupont Circle Spectrum Utilization During Peak Hours," The New America Foundation and The Shared Spectrum Company, Tech. Rep., 2003. [Online]. Available: "http://www.newamerica.net/Download_Docs/pdfs/Doc_File_183_1.pdf"

[3] J. P. Pavn, S. S. N, V. Gaddam, K. Challapali, and C. Chou, "The MBOA-WiMedia specification for ultra wideband distributed networks," *IEEE Communications Magazine*, vol. 44, no. 6, pp. 128 – 134, June 2006.

[4] R. Tandra and A. Sahai, "SNR walls for feature detectors," in *Proc. of the second IEEE International Symposium on New Frontiers in Dynamic Spectrum Access Networks, DySPAN*, 2007. [Online]. Available: "http://www.eecs.berkeley.edu/~tandra/pub1.htm"

[5] N. Hoven and A. Sahai, "Power scaling for cognitive radio," in *Proc. of the WirelessCom 05 Symposium on Signal Processing*, 2005. [Online]. Available: "http://www.eecs.berkeley.edu/~sahai/Papers/Niels_WirelessCom05.pdf"

[6] A. Sahai, N. Hoven, and R. Tandra, "Some Fundamental Limits on Cognitive Radio," in *Allerton Conference on Communication, Control, and Computing*, 2004. [Online]. Available: "http://www.eecs.berkeley.edu/~sahai/Papers/cognitive_radio_preliminary.pdf"

[7] C. Cordeiro, K. Challapali, D. Birru, and S. Shankar, "IEEE 802.22: the first worldwide wireless standard based on cognitive radios," in *Proc. of the first IEEE International Symposium on New Frontiers in Dynamic Spectrum Access Networks, DySPAN*, 2005.

[8] R. Tandra and A. Sahai, "Fundamental limits on detection in low SNR under noise uncertainty," in *Proc. of the WirelessCom 05 Symposium on Signal Processing*, 2005. [Online]. Available: "http://www.eecs.berkeley.edu/~sahai/Papers/Rahul_WirelessCom05.pdf"

[9] ——, "SNR walls for signal detection," 2008. [Online]. Available: "http://www.eecs.berkeley.edu/~tandra/pub1.htm"

[10] D. Cabric, A. Tkachenko, and R. Brodersen, "Experimental Study of Spectrum Sensing based on Energy Detection and Network Cooperation," in *Proc. of the ACM 1st International Workshop on Technology and Policy for Accessing Spectrum (TAPAS)*, 2006.

[11] S. Mishra, A. Sahai, and R. Brodersen, "Cooperative Sensing Among Cognitive Radios," in *Proc. of the IEEE International Conference on Communications (ICC)*, 2006.

[12] A. Sahai, D. Cabric, N. Hoven, S. M. Mishra, and R. Tandra, "Spectrum sensing: fundamental limits and practical challenges," in *Tutorial presented at the 1st IEEE Conference on Dynamic Spectrum Management (DySPAN05)*, 2005),.

[13] S. Gezici, "Localization via ultra-wideband radios," *IEEE Signal Processing Magazine*, July 2005.

[14] G. Atia, S. Aeron, E. Ermis, and V. Saligrama, "Cooperative Sensing in Cognitive Radios," in *Allerton Conference on Communication, Control, and Computing*, 2007.

[15] T. S. Rappaport, *Wireless Communications: Principles and Practice*. Prentice Hall, 2002.

[16] D. Tse and P. Viswanath, *Fundamentals of Wireless Communications*. Cambridge University Press, 2005.

[17] J. Kunisch and J. Pamp, "Measurement results and modeling aspects for the uwb radio channel," in *Ultra Wideband Systems and Technologies*, May 2002.

[18] "Digital Telivision/HDTV channel list: San Francisco Bay Area." [Online]. Available: "http://www.choisser.com/sfonair.html"

[19] G. Chouinard, "Dtv signal stochastic behavior at the edge of the protected contour and resulting probability of detection from various sensing schemes," IEEE 802.22 Meeting Documents, March 2007.